



# Laser ablation protection of polymer matrix composites by adhesive inorganic coatings

Guochao Chen<sup>1</sup> , Shizhen Zhu<sup>1,\*</sup> , Ze Jiang<sup>1</sup> , Lihong Gao<sup>1</sup> , Zhuang Ma<sup>1</sup> , and Ling Liu<sup>1</sup>

<sup>1</sup> School of Materials Science and Engineering, Beijing Institute of Technology, Beijing 100081, China

Received: 21 March 2017

Accepted: 17 July 2017

Published online:  
26 July 2017

© Springer Science+Business  
Media, LLC 2017

## ABSTRACT

Further utilization of polymer matrix composites (PMCs) in the aerospace industry is threatened by the development of laser weapons, resulting from weak oxidation resistance, low operation temperature and poor anti-laser ablation performance of the PMCs. Preparing an adhesive inorganic coating on the surface of components is an effective method to improve the laser irradiation resistance. Anti-laser ablation coatings composed of  $ZrO_2$  as pigment and sodium silicate as binder with different curing agents (including  $SiO_2$  and  $Na_2SiF_6$ ) are fabricated on the PMCs substrate with brush painting. Influence of the different curing agents on anti-laser ablation of the coatings at the laser wavelength of 1064 nm is investigated. The rear surface temperature of substrate with coatings, containing  $SiO_2$  and  $Na_2SiF_6$ , decreases from 240 to 60 and 70 °C, respectively, when testing at 1000 W for 5 s. After irradiation test at 1000 W for 10 s, the coating with  $SiO_2$  as curing agent shows slight molten state on the surface, while the coating with  $Na_2SiF_6$  is broke down, because coating containing  $SiO_2$  possesses more compact microstructure and fewer cracks than that with  $Na_2SiF_6$ .

## Introduction

Polymer matrix composites (PMCs) have been widely used in aerospace, marine and automobile industries during the past several decades resulting from their good engineering properties such as high specific strength and stiffness, lower density and so on [1, 2]. However, the further utilization of PMCs in aerospace industry is threatened by the rapid development of laser weapons, due to the weak oxidation resistance, low operation temperature and poor anti-laser ablation performance of the PMCs [3, 4]. It has

been authenticate that surface modification technologies enable to accomplish the feasibility and efficiency of protecting the PMCs substrates [5]. Technologies, including electroplating, thermal spraying [6, 7], physical vapor deposition (PVD) [8, 9], chemical vapor deposition (CVD) [10, 11] and electroless plating [12–14] technologies, are comprehensively applied to manufacture various coatings on the substrate materials, which are propitious to drive up the performance, extend the lifetime and expand the application field. Researches indicate that the high reflectance of optical films helps to decrease the

Address correspondence to E-mail: zhusz@bit.edu.cn

absorption of the laser power and protect the substrate materials from damage [15, 20]. Nevertheless, optical films are difficult to be applied on the complex-shaped substrate and can be easily contaminated [16–18]. In contrast, brush painting, as a kind of typical adhesive coating technology, is considered an appropriate candidate to prepare protective coating because of its easy operation and suitable use in complex shape and large size for substrates.

In general, a typical inorganic binder, such as sodium silicate, plays an important role in adhesive coating process, and it is widely employed in the extreme condition of high temperature and laser irradiation [19]. Besides,  $ZrO_2$  exhibits excellent properties, such as high reflectance, high oxygen storage capacity, low thermal conductivity, high thermal shock resistance, high fracture toughness, high-temperature phase stability and chemical durability, which meet the requirements of the substrate materials and the functional coatings [20–22]. Recently, most studies focus on the materials irradiated by the low-energy laser or for short time [23–25]. There are rarely studies focusing on the high energy continuous laser protection of carbon fiber-reinforced polymer matrix composites (Cf/PMCs).

This paper chooses sodium silicate as binding agent, silicon oxide or sodium fluorosilicate as curing agent and zirconium oxide as filler. The inorganic materials with excellent heat insulation performance and high reflectivity at the wavelength of 1064 nm were selected as addition to improve ablation resistance of coating.  $ZrO_2$ –sodium silicate coating on the surface of Cf/PMCs substrate was prepared by brush painting and sequential drying treatment. In this work, the objective of this study was to investigate the laser ablation resistance of the inorganic coating. Some critical performances such as reflectance and the heat resistance of the coatings at the laser wavelength of 1064 nm were studied. As well, the microstructures of the coatings before and after property testing were discussed. Furthermore, laser ablation and laser-proof mechanisms of coating were explored.

## Experimental method

### Sample preparation

The size of commercial substrate of Cf/PMCs was 50\*50\*2 mm. For the sake of getting significant

bonding between substrate and coating, the substrate should be sandpaper coarsened, activated and washed with deionized water before brush painting. The ceramic slurry was prepared using commercial powders listed as followings:  $ZrO_2$  (Alfa Astar, USA, particle size 0.1–0.3  $\mu\text{m}$ , 99%),  $SiO_2$  (Alfa Astar, USA, 30–50  $\mu\text{m}$ , 99%) and  $Na_2SiF_6$  (Alfa Astar, USA, 40–60  $\mu\text{m}$ , 99%). The sodium silicate with modulus of 2.7 and Baume degree of 48 was selected as binding agent. The raw materials were firstly weighted according to the formulation, listed in Table 1, and then milled for 10 min with a rate of 1000 r/min. Then, the substrates were coated with ceramic slurry by brush painting with the scraper and groove to get a coating about 1 mm in thickness. After scraping, the samples were dried at room temperature for 12 h, at 323 K for 8 h, 373 K for 8 h, 473 K for 4 h and 523 K for 4 h in turn to make the coating sufficiently cure.

### Laser irradiation tests

The laser ablation tests in this paper were carried out by using yttrium laser system (YSL-2000) with the wavelength of 1064 nm in atmospheric environment. The spot size of the Gaussian laser was set as about 10 mm  $\times$  10 mm, and the laser power was variable at three levels of 500, 1000 and 1500 W. The samples were irradiated by laser for 5 or 10 s. During the laser irradiation, the intensity of forward-scattered light (FSL) of coating was measured by IR receiver (GD3561T, China). Meanwhile, the rear surface temperature of sample in the center region was synchronously measured by K-type thermocouple.

### Characterization

The surface roughness of raw coatings was measured by Surface Roughness gauge (pocket era TR100, USA). The reflectivity of raw coatings was measured by Cary 5000 Ultraviolet -Visible-Infrared spectrophotometer with the condition of room temperature and weak light. Tensile test was carried out for the coatings using a tensile testing instrument

**Table 1** The formulations of coatings

Sample	$ZrO_2$ (g)	$SiO_2$ (g)	$Na_2SiF_6$ (g)	Sodium silicate (g)
S1	5	5	0	5
S2	5	0	5	5

(WDW-E100D, China). Tensile test samples were machined to be  $\Phi 25.4 \times 3$  mm and glued (914 epoxy resin) with mating part of same dimension. Cross-head speed of 1 mm/min was applied for all coatings. The phase structure and surface microstructure of the samples before and after irradiation were examined by scanning electron microscope (SEM, Hitachi S4800, Japan). The composition of the samples was identified by energy-dispersive spectroscopy (EDS, Oxford, G.B.). The mass ablative rate ( $M$ ) was computed using Eq. (1).

$$M = \frac{m_o - m_t}{\Delta t} \quad (1)$$

where  $m_o$  and  $m_t$  are mass of samples (in grams) before and after irradiation test,  $\Delta t$  is total time of laser irradiation (in seconds).

## Results and discussion

### Morphology and characteristics

According to the repeated five times of tensile test, the average adhesive bond strength of S1 is 3.56 MPa. That of S2 is 3.24 MPa. For both samples, the fracture occurred on the interface, which indicates that the cohesive bond strength of coating is higher than the obtained adhesive bond strength. Figure 1 shows the reflectivity spectra of coatings of S1 and S2 before laser irradiation. The reflectivity of both samples is about 95% at the wavelength of 1064 nm. However, the surface roughness of S1 is Ra 2.38  $\mu\text{m}$ , and that of S2 is Ra 3.57  $\mu\text{m}$ . The reasons may be explained by the surface micro-morphology before being ablated, as shown in Fig. 2. The surface of S1 is more compact,

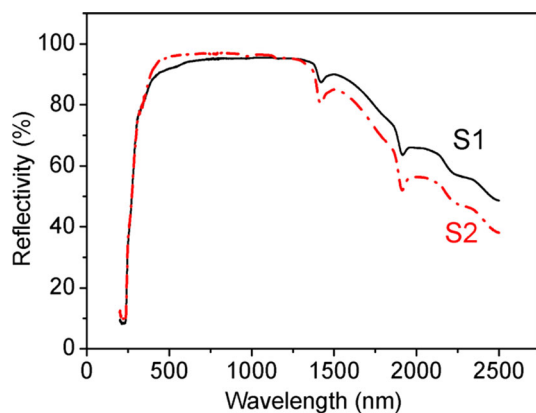


**Figure 1** Reflectivity spectra of coatings before laser irradiation.

whose cracks are finer. Because of faster curing rate of coating with sodium fluorosilicate, the outmost surface firstly tends to cure, then the inner vapor gathers in one place and volatilizes when the temperature increasing, resulting in the cracks and pits.

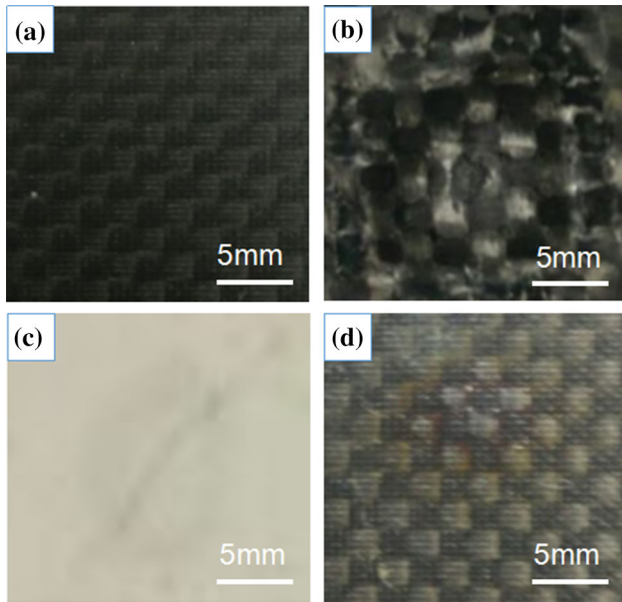
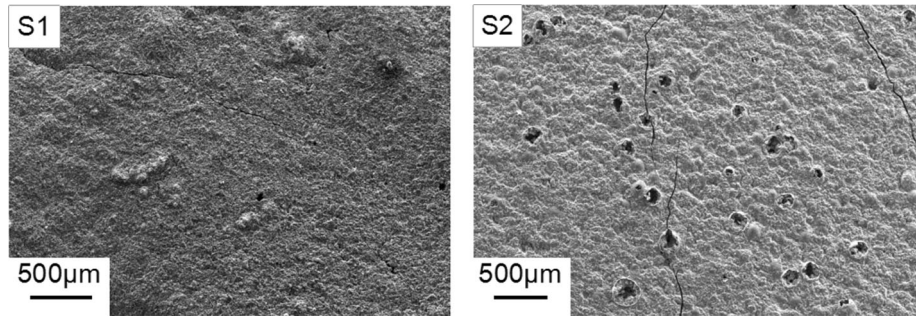
### Ablation resistance performance

Figure 3 describes the macroscopic front surface state of the substrates and coatings before or after laser irradiation. The original surface of Cf/PMCs substrate before irradiation is exhibits in Fig. 3a. After being irradiated by the laser with energy of 1000 W for 5 s, the surface state of the substrate without coating was significantly damaged and the mass ablative rate ( $M$ ) of substrate was  $0.026 \text{ g s}^{-1}$ . According to Fig. 3b, it can be seen that the cross-woven carbon fiber exposed obviously, carbon fiber occurring oxidizing ablation and resin was ablated seriously. However, slight ablation marks were found on the coating of S1 under the condition of 1000 W laser irradiation for 5 s, whose ablation area is about  $25 \text{ mm}^2$ , as shown in Fig. 3c. After soaking this S1 sample in water for 7 days and sequentially scraping coating off manually, the front surface state of S1 substrate is shown in Fig. 3d. It is revealed that front surface of S1 substrate is slightly affected by heat transmitted from the coating and still remains intact.

The rear surface temperature of substrate without coating significantly rose during laser irradiation with the energy of 1000 W for 5 s. After the laser irradiated for 5 s, the rear surface temperature of substrate still rose and finally reached up to the highest temperature of  $240 \text{ }^\circ\text{C}$ , because the energy of laser was transferred by heat. While the rear surface temperature of S1 rose slowly, the highest temperature of S1 was  $60 \text{ }^\circ\text{C}$  during the same laser irradiation. When the laser irradiation was over, the rear surface temperature of substrate no longer rose, indicating the significant thermal resistance of the coating of S1 sample. While, the highest temperature of S2 was  $70 \text{ }^\circ\text{C}$ , whose rate of rise of temperature was higher than that of S1, suggesting that the thermal insulation of S2 be inferior to that of S1, as shown in Fig. 4.

The intensity of forward-scattered light (FSL) of coating was much higher than that of substrate without coating, and the intensity was stable, as shown in Fig. 5. The deposition and transmission of

**Figure 2** Surface micro-morphology of coatings before laser irradiation.



**Figure 3** Macroscopic front surface state of **a** substrate before irradiation, **b** substrate after irradiation, **c** coating of S1 after irradiation and **d** substrate of S1 after irradiation with laser energy of 1000 W for 5 s.

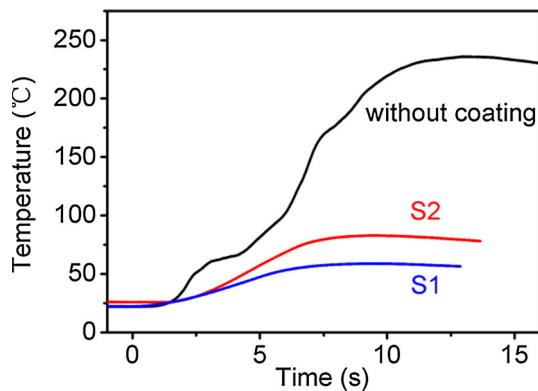


**Figure 4** Rear surface temperature of different samples during laser irradiation with energy of 1000 W for 5 s.

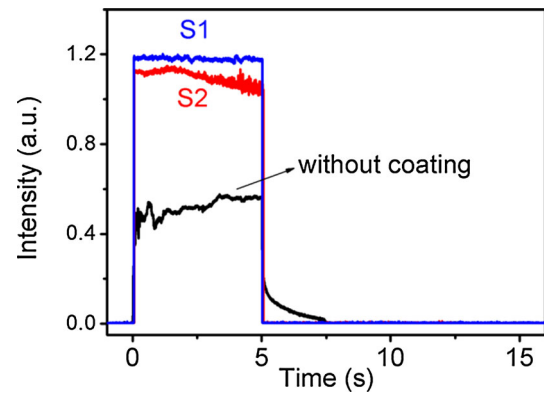


**Figure 5** FSL intensity of different samples during laser irradiation with energy of 1000 W for 5 s.

laser energy can be prevented resulting from high intensity of FSL of coating.

When the power of laser was 500 W for 10 s, there was no evident ablation region on the coating, as shown in Fig. 6a. When the power of laser was 1000 W for 10 s, there was obviously milk white ablation region on the coating, and the ablation area was about 78.5 mm<sup>2</sup>, as shown in Fig. 6b. When the power of laser was 1500 W for 10 s, the coating of central area of irradiation disappeared entirely because of higher energy, as shown in Fig. 6c. The edge area of irradiation contracted to develop bright white raised area, and the ablation area was about 176.6 mm<sup>2</sup>.

The macroscopic appearance of S1 and S2 which were irradiated by laser with energy of 1000 W for 10 s was compared, as shown in Fig. 6b, d. During the laser irradiation, S2 generated splash and dark smoke, and the coating was broken down because of thermomechanical coupling effects. The ablation area was about 100.1 mm<sup>2</sup>. Some cracks were perpendicular to the edge of ablation zone there. The laser

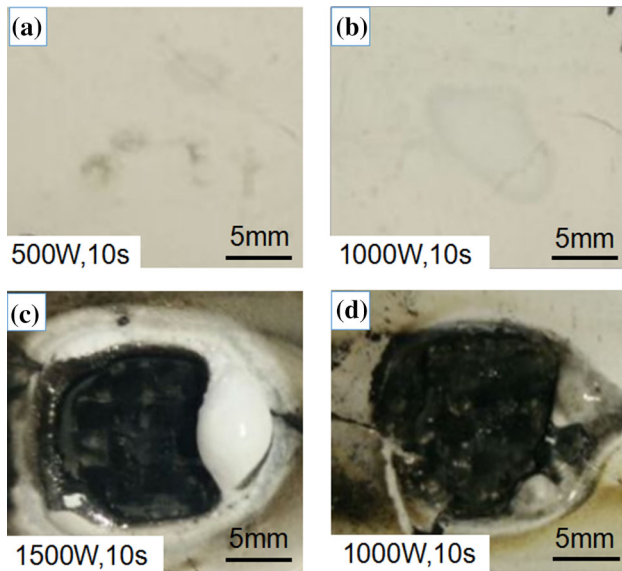


**Figure 6** Macroscopic surface state of (a–c) S1 coating (d) and S2 coating for different laser irradiation parameters.

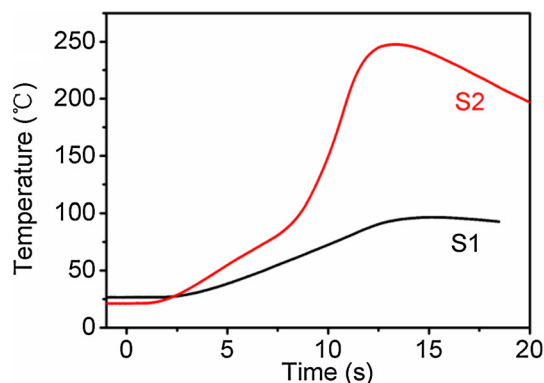


**Figure 7** Rear surface temperature of different samples during laser irradiation with energy of 1000 W for 10 s.

energy imparted to the sample during the laser irradiation was sufficient to induce thermal stresses on the coating surface that resulted in dissemination of existing macrocracks.

Figure 7 describes the relation between the rear surface temperature of samples and time with the laser energy of 1000 W irradiated for 10 s. The rear surface temperature of S1 increased slowly, and the highest temperature was about 100 °C. However, the rear surface temperature of S2 increased rapidly. There was a sharp increase in the rate of rise of temperature at the 5th second after laser opening, possibly because the coating was broken down at the moment. The temperature of substrate rose

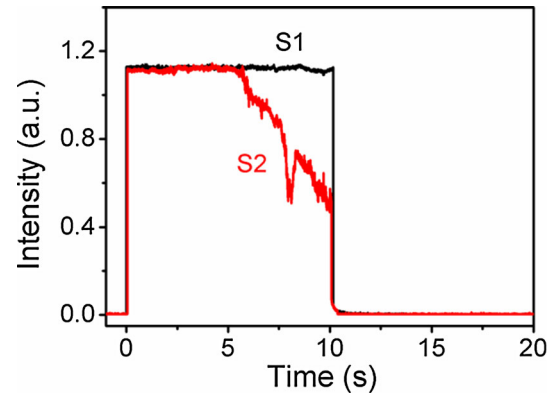
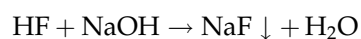
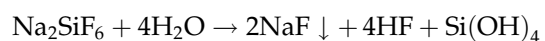


**Figure 8** FSL intensity of different samples during laser irradiation with energy of 1000 W for 10 s.

dramatically without the insulating effect and high reflectivity of coating to consume laser energy. The highest temperature was about 240 °C. FSL of both samples was similar in first 5 s after laser opening. FSL of S2 decreased sharply at the 5th second after laser opening due to laser energy deposition during the laser irradiation, so the coating was broken down, as shown in Figs. 6d and 8.

Surface of S1 showed slight molten state by the laser with energy of 1000 W for 10 s, as shown in Fig. 9. What are the reasons for the difference of laser irradiation resistance between these two kinds of coating? There were some pits on the surface of S2, as shown in Fig. 2. Much more laser energy could be absorbed because of the pits, and then temperature in some local areas got so high to start physical or chemical reactions. The coating was broken down due to the propagation of cracks and other defects. However, the sample whose curing agent is silicon dioxide is denser and owns fewer defects. In addition, sodium fluorosilicate begins to decompose at 300 °C around, which damages the compactness of coating resulting in the absorption of more laser energy, while silicon dioxide itself has good thermal stability. Furthermore, sodium fluoride in the coating of S2 samples was produced by the following reaction between sodium fluoride as curing agent and sodium silicate binder during the curing process.



For S2 sample, sodium fluoride melting point of precipitate sodium fluoride is around 993 °C and is obviously lower than that of silicon dioxide, so more

**Figure 9** Microscopic morphology of S1 (a) before (b) and after laser irradiation with energy of 1000 W for 10 s.

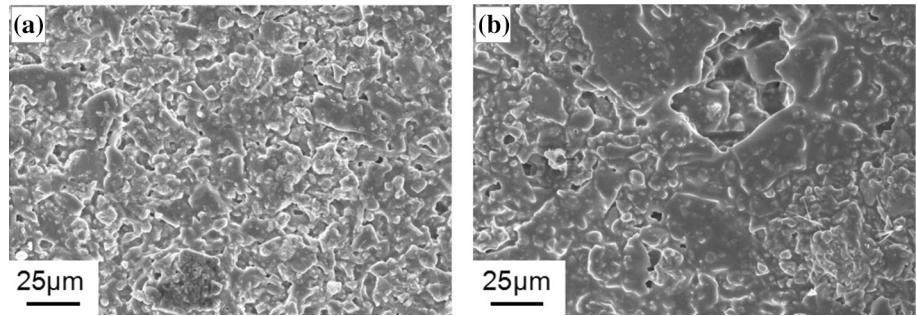


**Figure 10** Microscopic morphology of ablation central area of S1 after laser irradiation with energy of 1000 W for 10 s.

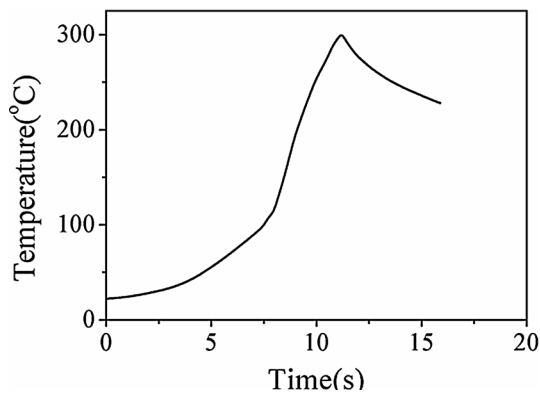
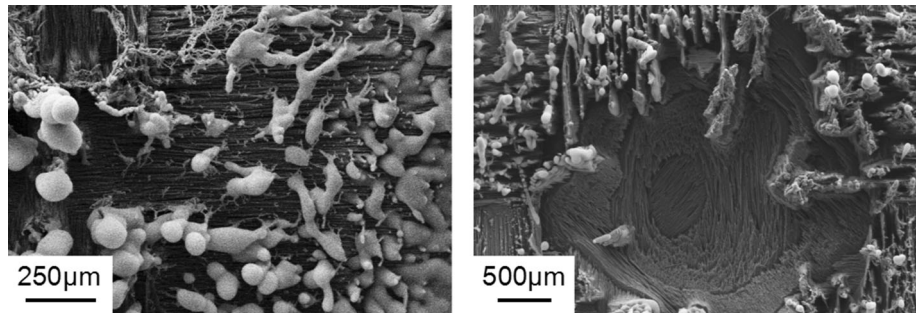


**Figure 11** Rear surface temperature of S1 after laser irradiation with energy of 1500 W for 10 s.

severe mass loss and larger size pores, observed in Fig. 9, come into being before laser irradiation.

### Ablation mechanism

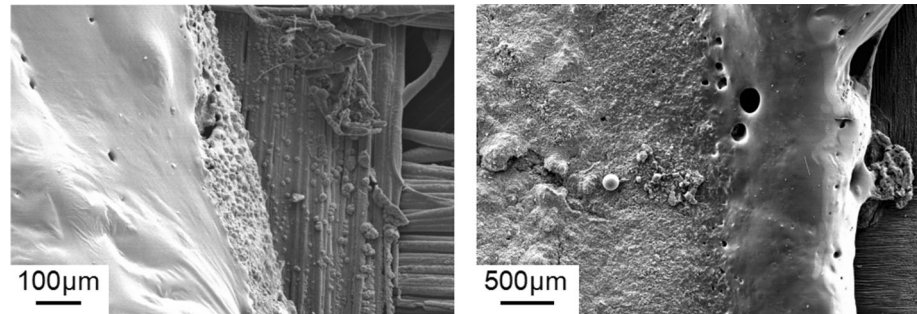
Under the effect of laser thermal shock, central area of laser irradiation of S1 occurred serious ablation, as shown in Fig. 10. Resin decomposition and carbon fibers oxidation of substrate were caused, as a result of coating's melting and gasifying when laser irradiating to produce a high-temperature area. Some bright white nearly spherical particles distributing around the edge of the pit are mainly composed of Zr



**Figure 12** Macroscopic morphology of S1 rear surface after laser irradiation with energy of 1500 W for 10 s.

and O by means of EDS analysis, generated by melting of  $ZrO_2$  particles. The rising process of rear surface temperature can be divided into two stages, as shown in Fig. 11. Firstly, the temperature slowly rises, since that the coating owns good insulating ability and high reflectivity. What is more, coating can consume laser energy by melting and gasifying. With laser energy continuous deposition, the coating was broken down at the 7th second after laser opening, and the protective effect disappearing, so the temperature rapidly rises. The highest rear surface temperature of substrate is 300 °C. The rear

**Figure 13** Microscopic morphology of ablation edge area of S1 after laser irradiation with laser energy of 1500 W for 10 s.



surface of substrate slightly turned yellow, and resin is slightly ablated to decompose at this temperature, as shown in Fig. 12.

Figure 13 describes the microstructure of edge area of S1 irradiated by laser energy of 1500 W for 10 s. There are little Zr on the surface of fringe area, but a lot of Si and Na from EDS analysis. We can conclude that the surface of edge area is covered by molten silicon oxide and sodium oxide, as well  $ZrO_2$  particles are covered. This kind of structure possesses fine insulating effect. There are some circular cavities on the surface of edge area resulting from melting and gasifying of sodium silicate at high temperature.

## Conclusion

The inorganic coating prepared on  $C_f$ /PMCs achieves protection mechanism of non-ablating, thermal insulation and high reflectivity at the wavelength of 1064 nm. This coating effectively protects the  $C_f$ /PMCs substrate from laser irradiating. With the increase in laser power and irradiation time, the continual deposition of laser energy leads to the temperature rise of coating. Damaging process of coating includes melting and gasifying of sodium silicate, silicon oxide and zirconium oxide.

The rear surface temperature of substrate with coatings, containing  $SiO_2$  and  $Na_2SiF_6$ , decreased from 240 to 60 and 70 °C, respectively, when testing at 1000 W for 5 s. The coating with sodium silicate as binding agents, silicon oxide as curing agent, zirconium oxide as filler shows slight molten state on the surface irradiated by the laser with energy of 1000 W for 10 s, while the coating with sodium fluorosilicate as curing agent is broke down, because the coating with silicon dioxide as curing agent is denser and owns fewer defects, and silicon dioxide itself has good thermal stability, which improves the laser

irradiation resistance of coating. Sodium fluorosilicate begins to break down at 300 °C, which damages the compactness of coating resulting in the absorption of laser energy.

## Acknowledgements

The use of the National Key Laboratory of Science and Technology on Armor and Anti-armor Materials at BIT is gratefully acknowledged. The authors would like to acknowledge the Wenzhi Li and Jiayi Zheng for their contributions in polishing this paper.

## References

- [1] Zhong ZL, Li MY, Liao ZD, Lu LL (2016) The impact of adhesive resin solution on carbon fibers cloth and jute-reinforced epoxy resin matrix composites. *J Text Inst* 107:1264–1267
- [2] Guo H, Huang YD, Liu L, Shi XH (2010) Effect of epoxy coatings on carbon fibers during manufacture of carbon fiber reinforced resin matrix composites. *Mater Des* 31:1186–1190
- [3] Li J, Guan ZW, Zhang YZ, Wang Y, Wang ZY (2014) Laser ablation resistance behavior of organosilicone composite coating on various substrates. *Mater Sci Forum* 789:461–465
- [4] Chen Z, Cheng H, Tao J, Wan S, Wu W (2009) Influence of irradiation time on laser ablation behavior of polycarbosilanes coating. *J Polym Eng* 29:385–393
- [5] Li J (2008) Interfacial studies on the  $O_3$  modified carbon fiber-reinforced polyamide 6 composites. *Appl Surf Sci* 255:2822–2824
- [6] Arai M, Ochiai H, Suidzu T (2016) A novel low-thermal-conductivity plasma-sprayed thermal barrier coating controlled by large pores. *Surf Coat Technol* 285:120–127
- [7] Qing YC, Su JB, Wen QL, Luo F, Zhu DM, Zhou WC (2015) Enhanced dielectric and electromagnetic interference shielding properties of  $FeSiAl/Al_2O_3$  ceramics by plasma spraying. *J Alloys Compd* 651:259–265

- [8] Yang W, Xiong J, Guo ZX, Du H, Yang TN, Tang J, Wen B (2017) Structure and properties of PVD TiAlN and TiAlN/CrAlN coated Ti(C, N)-based cermets. *Ceram Int* 43:1911–1915
- [9] Skordaris G, Bouzakis KD, Kotsanis T, Charalampous P, Bouzakis E, Lemmer O, Bolz S (2015) Film thickness effect on mechanical properties and milling performance of nanostructured multilayer PVD coated tools. *Surf Coat Technol* 307:452–460
- [10] Sun N, Wang C, Jiao L, Zhang J, Zhang D (2017) Controllable coating of boron nitride on ceramic fibers by CVD at low temperature. *Ceram Int* 43:1509–1516
- [11] Toller L, Liu C, Holmström E, Larsson T, Norgren S (2017) Investigation of cemented carbides with alternative binders after CVD coating. *Int J Refract Met Hard* 62:225–229
- [12] Yim YJ, Rhee KY, Park SJ (2015) Influence of electroless nickel-plating on fracture toughness of pitch-based carbon fibre reinforced composites. *Compos Part B Eng* 76:286–291
- [13] Liu Z, He F, Gao F, Ren B, Huang Y (2016) Fabrication and electromagnetic properties of novel FeNi alloy-coated flake graphite prepared by electroless plating. *J Alloys Compd* 656:51–57
- [14] Park SJ, Ko TJ, Yoon J, Moon MW, Oh KH, Han JH (2017) Copper circuit patterning on polymer using selective surface modification and electroless plating. *Appl Surf Sci* 396:1678–1684
- [15] Zhang J, Bu X, Ma B, Jiao H, Cheng X, Wang Z (2017) Research on the mechanical stability of high laser resistant coatings on lithium triborate crystal. *Appl Opt* 57:117–122
- [16] Zou Y, Zhao LL, You LJ, Chen XY, Song LX (2016) Preparation and numerical simulation investigation of high reflectance anti-laser-ablation coating. *J Inorg Mater* 31:869–875
- [17] Langlet M, Burgos M, Coutier C, Jimenez C, Morant M Manso (2001) Low temperature preparation of high refractive index and mechanically resistant sol–gel TiO<sub>2</sub> films for multilayer antireflective coating applications. *Sol Gel Sci Technol* 2:695–705
- [18] Sta I, Jlassi M, Hajji M, Boujmil MF, Jerbi R, Kandyla M, Kompitsas M, Ezzaouia H (2014) Structural and optical properties of TiO<sub>2</sub> thin film prepared by spin coating. *J Sol Gel Sci Technol* 72:421–427
- [19] Kumar SP, Takamori S, Araki H, Kuroda S (2015) Flame retardancy of clay–sodium silicate composite coatings on wood for construction purposes. *RSC Adv* 5:34109–34116
- [20] Huang W, Cheng H, Zhang C, Zhou Y, Cao X (2015) Thermal ablation of stabilized zirconia/metal coated polyimide matrix composites via plasma spray process. *Plasma Chem Plasma Process* 35:587–603
- [21] Balagna C, Perero S, Ferraris S, Miola M, Fuciale G, Manfredotti C, Battiato A, Santella D, Verne E, Vittone E, Ferraris M (2012) Antibacterial coating on polymer for space application. *Mater Chem Phys* 135:714–722
- [22] Wu DS, Lo WC, Chiang CC, Lin HB, Chang LS, Horng RH, Huang CL, Gao YJ (2005) Water and oxygen permeation of silicon nitride films prepared by plasma-enhanced chemical vapor deposition. *Surf Coat Technol* 198:114–117
- [23] Liu N, Wang YJ, Zhou M, Jing XF, Wang YZ, Cui Y, Jin YX (2010) Laser resistance of Ta<sub>2</sub>O<sub>5</sub>/SiO<sub>2</sub> and ZrO<sub>2</sub>/SiO<sub>2</sub> optical coatings under 2 μm femtosecond pulsed irradiation. *Chin Phys Lett* 27:074215
- [24] Yan ZY, Ma Z, Liu L, Zhu SZ, Gao LH (2014) The ablation behavior of ZrB<sub>2</sub>/Cu composite irradiated by high-intensity continuous laser. *J Eur Ceram Soc* 34:2203–2209
- [25] Li X, Liu XF, Zhao YA, Shao JD, Fan ZX (2010) Laser-conditioning mechanism of ZrO<sub>2</sub>/SiO<sub>2</sub> HR films with fitting damage probability curves of laser-induced damage. *Chin Opt Lett* 8:598–600